World Journal of Radiology

Submit a Manuscript: http://www.wjgnet.com/esps/
Help Desk: http://www.wjgnet.com/esps/helpdesk.aspx
DOI: 10.4329/wjr.v8.i6.618

*World J Radiol* 2016 June 28; 8(6): 618-627
ISSN 1949-8470 (online)


ORIGINAL ARTICLE

Prospective Study

# Assessment of sub-milli-sievert abdominal computed tomography with iterative reconstruction techniques of different vendors

Atul Padole, Nisha Sainani, Diego Lira, Ranish Deedar Ali Khawaja, Sarvenaz Pourjabbar, Roberto Lo Gullo, Alexi Otrakji, Mannudeep K Kalra

Atul Padole, Nisha Sainani, Diego Lira, Ranish Deedar Ali Khawaja, Sarvenaz Pourjabbar, Roberto Lo Gullo, Alexi Otrakji, Mannudeep K Kalra, Department of Radiology, Massachusetts General Hospital, Boston, MA 02114, United States

Nisha Sainani, Department of Radiology, Brigham and Women's Hospital, Boston, MA 02115, United States

Author contributions: Padole A, Khawaja RDA and Pourjabbar S were involved in patient recruitment and objective measurement; Padole A and Kalra MK wrote the manuscript; Sainani N and Lira D were the readers of the study; Lo Gullo R and Otrakji A were involved in blinding of study; Kalra MK helped in consenting patients and designing the study.

Institutional review board statement: The Human Research Committee of our Institutional Review Board (IRB) approved this Health Insurance Portability and Accountability Act (HIPAA) compliant prospective clinical study.

Informed consent statement: All study participants provided informed written consent prior to study enrollment.

Conflict-of-interest statement: None of the authors have any pertinent financial disclosures.

Data sharing statement: All the study participants gave written informed consent for data sharing.



Correspondence to: Atul Padole, MD, Department of Radiology, Massachusetts General Hospital, Harvard Medical School, 25 New Chardon St, 4th Floor, Boston, MA 02114, United States. apadole@mgh.harvard.edu
Telephone: +1-617-6435076
Fax: +1-617-6430111

Received: November 28, 2015
Peer-review started: November 30, 2015
First decision: December 28, 2015
Revised: January 8, 2016
Accepted: March 7, 2016
Article in press: March 9, 2016
Published online: June 28, 2016

## Abstract

**AIM:** To assess diagnostic image quality of reduced dose (RD) abdominal computed tomography (CT) with 9 iterative reconstruction techniques (IRTs) from 4 different vendors to the standard of care (SD) CT.

**METHODS:** In an Institutional Review Board approved study, 66 patients (mean age 60 ± 13 years, 44 men, and 22 women) undergoing routine abdomen CT on multi-detector CT (MDCT) scanners from vendors A, B, and C (≥ 64 row CT scanners) (22 patients each) gave written informed consent for acquisition of an additional RD CT series. Sinogram data of RD CT was reconstructed with two vendor-specific and a vendor-neutral IRTs (A-1, A-2, A-3; B-1, B-2, B-3; and C-1, C-2, C-3) and SD CT series with filtered back projection. Subjective image evaluation was performed by two radiologists for each SD and RD CT series blinded and independently. All RD CT series (198) were assessed first followed by SD CT series (66). Objective image noise was measured for SD and RD CT series. Data were analyzed by Wilcoxon signed rank, kappa, and analysis of variance tests.

**RESULTS:** There were 13/50, 18/57 and 9/40 missed lesions (size 2-7 mm) on RD CT for vendor A, B, and C, respectively. Missed lesions includes liver cysts, kidney cysts and stone, gall stone, fatty liver, and pancreatitis. There were also 5, 4, and 4 pseudo lesions (size 2-3 mm) on RD CT for vendor A, B, and C, respectively. Lesions conspicuity was sufficient for clinical diagnostic performance for 6/24 (RD-A-1), 10/24 (RD-A-2), and 7/24 (RD-A-3) lesions for vendor A; 5/26 (RD-B-1), 6/26 (RD-B-2), and 7/26 (RD-B-3) lesions for vendor B; and 4/20 (RD-C-1) 6/20 (RD-C-2), and 10/20 (RD-C-3) lesions for vendor C ($P$ = 0.9). Mean objective image noise in liver was significantly lower for RD A-1 compared to both RD A-2 and RD A-3 images ($P$ < 0.001). Similarly, mean objective image noise lower for RD B-2 (compared to RD B-1, RD B-3) and RD C-3 (compared to RD C-1 and C-2) ($P$ = 0.016).

**CONCLUSION:** Regardless of IRTs and MDCT vendors, abdominal CT acquired at mean CT dose index volume 1.3 mGy is not sufficient to retain clinical diagnostic performance.

**Key words:** Adult; Computed tomographic imaging; Abdomen; Radiation dose



**Core tip:** We assessed the performance of abdominal computed tomography (CT) acquired at sub-milli-Sievert radiation dose to the standard of care CT. A total of 66 subjects were scanned on three different multi-detector CT scanners at sub-milli-Sievert radiation dose [or CT dose index volume ($CTDI_{vol}$) of 1.3 mGy]. Images were reconstructed with vendor-specific and vendor-neutral iterative reconstruction techniques (IRTs). We compared the clinical diagnostic performance of vendor specific and vendor neutral IRTs at sub-milli-Sievert radiation dose to the standard of care CT. We found that regardless of the IRTs and multi-detector CT vendors, $CTDI_{vol}$ of 1.3 mGy or sub-mill-sievert radiation dose did not provide sufficient clinical diagnostic performance for abdominal CT.

Padole A, Sainani N, Lira D, Khawaja RDA, Pourjabbar S, Lo Gullo R, Otrakji A, Kalra MK. Assessment of sub-milli-sievert abdominal computed tomography with iterative reconstruction techniques of different vendors. *World J Radiol* 2016; 8(6): 618-627 Available from: URL: http://www.wjgnet.com/1949-8470/full/v8/i6/618.htm DOI: http://dx.doi.org/10.4329/wjr.v8.i6.618

## INTRODUCTION

Due to increase in use of computed tomography (CT) examinations in modern medicine, appropriate use of CT radiation dose has become paramount. Several strategies have been employed to enable radiation dose reduction. These strategies include scanning with lower tube current or voltage, use of automatic exposure control (AEC) technique, image processing and reconstruction techniques such as noise reduction filters and iterative reconstruction techniques (IRTs)[1-4].

With decrease in CT radiation dose, image noise and artifacts can increase. Conventional filtered back projection (FBP) is associated with higher image noise and possible artifacts with reduced dose (RD) CT. IRTs help to improve image quality in RD CT examinations[5-9].

IRT may be classified into two broad groups, vendor-specific IRT which can only reconstruct images for specific vendor CT scanner and vendor-neutral IRT which can reconstruct images from any scanner or vendor. Prior studies have assessed use of vendor-specific IRTs for reducing radiation dose associated with abdomen CT without compromising image quality[5-9]. In this study, we performed the image quality assessment RD abdominal CT on multi-detector CT (MDCT) scanners of different vendors. We assessed nine different IRTs from four different IRTs vendors for RD (sub-milli-sievert) abdominal CT. The purpose of our study was to assess diagnostic image quality of RD abdominal CT with 9 IRTs from 4 different IRTs vendors to the standard of care CT (SD CT).

## MATERIALS AND METHODS

### *Patients*

None of the authors have any pertinent financial disclosures. The Human Research Committee of our Institutional Review Board approved this Health Insurance Portability and Accountability Act compliant prospective clinical study.

Sixty six patients (mean age 60 ± 13 years, 44 men, and 22 women) undergoing routine abdomen CT exams (enhanced or non-enhanced) on MDCT scanners from vendors A, B, and C (≥ 64 row CT scanners) (22 patients each) gave written informed consent for acquisition of an additional RD CT series. The MDCT Scanners used in our study included Siemens (SOMATOME Definition Flash, Germany), Philips (Brilliance iCT 256, Andover, MA), and GE (Discovery CT750 HD, Waukesha, WI) (in randomized order to protect identity of the scanners). The RD CT image series was acquired immediately (within 5-10 s) after acquisition of their SD CT series. The most common indications for SD CT in the recruited human subjects were abdominal pain, cancer staging, and unexplained weight loss. Inclusion criteria of study were adult patients (age > 18 years) who were hemodynamically stable, able to communicate in English, follow simple instructions and hold their breath for 10 s or longer. Patients undergoing urgent CT, or with known contrast allergy, women with on-going pregnancy or planning to get pregnant were excluded from the study. Hemodynamically unstable patients were also excluded. Weight and height measurements of patients were used to calculate body mass index (BMI, $kg/m^2$). Cross-sectional measurements (anteroposterior and lateral diameters) at mid-slice location were recorded for all

patients. Effective diameter was calculated by obtaining square root of product of anteroposterior and lateral diameters of the abdomen.

### *Scanning techniques*

Patients were instructed to avoid any voluntary movements during CT scanning. Patients were iso-centered in the gantry and planning radiographs (anteroposterior and lateral) were acquired at 120 kV and 20 mA. First, clinically indicated SD abdominal CT examination (with tube current modulation) was performed on MDCT scanners (vendor A, B, and C). For contrast enhanced exam, intravenous contrast agent (80-100 mL of Iopamidol 370 mg % Bracco Diagnostics, Princeton, NJ) was administered. Only one additional series of RD CT was acquired. The most RD CT exams were acquired before delayed CT series in contrast enhanced CT exams. Additional RD abdominal CT series (at fixed tube current) with identical scan length was acquired immediately after the SD CT. To minimize interval between SD and RD CT image series, both image series were planned prior to scan initiation. The average delay between SD and RD CT image acquisition was 5-10 s.

For RD CT series, dose length product (DLP) was kept $\leqslant$ 65 mGy*cm (estimated effective dose < 1 mSv) over the same scan length as the SD CT. DLP $\leqslant$ 65 mGy*cm was obtained with lower fixed tube current. However, SD CT was acquired with automatic tube current modulation technique with 100-120 kV. All other scanning parameters of RD CT series were kept identical to the SD CT including helical acquisition mode, gantry rotation time of 0.5 s, pitch 0.9-1.1, and reconstructed section thickness of 5 mm. CT dose index volume ($CTDI_{vol}$) and DLP were recorded from the dose information pages. Estimated effective dose for SD and RD abdominal CT were calculated by multiplying the DLP with 0.015 mSv/mGy*cm[10,11].

### *Image reconstruction*

The sinogram data of RD CT was reconstructed with two vendor-specific IRTs and a vendor - neutral IRT (4$^{th}$ vendor - SafeCT, Medic Vision, Israel) (A-1, A-2, A-3 for vendor A, B-1, B-2, B-3 for B, and C-1, C-2, C-3 for C). Vendor-specific IRTs include hybrid IRTs (blend with FBP) and pure IRTs (does not blend with FBP). Vendor-neutral IRTs images were generated from RD FBP series of vendor A, B, and C. Thus, image reconstructions were obtained for 9 different IRTs (3 IRTs/patient) reconstructed from the sinogram data of RD CT of vendor A, B, and C. Vendor specific IRT cannot be applied to CT data from other vendors or scanners. SD CT series for all patients were reconstructed with FBP. All image series ($n$ = 4 series per patient × 66 patients = 264 total image series) were evaluated for subjective image quality.

All CT series were evaluated on a DICOM image viewer ClearCanvas workstation (ClearCanvas Inc., Toronto, Canada). Subjective image quality evaluation was performed in a blinded, independent, and randomized manner. Both radiologists as well as study coordinator overseeing the interpretation were blinded to the identity of IRTs. Specific code names were given to all 9 IRTs of vendor A, B, and C. In a two-step procedure, blinding and randomization was conducted. A study co-investigator (R.L., not part of patient recruitment or evaluation sessions) coded and blinded all image series. Then, co-investigator (A.O., again not part of patient recruitment and evaluation sessions) coded and blinded the image series without knowledge of the first coding sequences.

Abdomen CT examinations of two patients were used for training the radiologists and were not included in data analysis. Images were assessed in abdominal window settings (window width = 400, window level = 40). Both radiologists were allowed to adjust the window settings.

### *Subjective image quality evaluation*

Two radiologists (N.S.: 12 years of experience, D.L.: 5 years of experience) independently evaluated all image series. Subjective image quality evaluation was performed for each SD and RD CT series independently. All RD CT series were assessed first followed by SD CT. All 264 (198 RD + 66 SD) image series of 66 patients were blinded and randomized separately.

One out of three IRTs (3 IRTs/patient) was initially displayed in a randomized order for evaluation of lesion detection, lesion conspicuity, and visibility of normal abdominal structures. Subsequently, other two IRTs were shown for subjective image quality evaluation. After evaluation of all RD CT image series, finally, SD CT series were evaluated to record "true positive" lesions and findings. Any lesion detected on SD CT but not on RD CT images was considered as "missed lesion". Any lesion not seen on SD but detected on RD CT was considered as "pseudo or false positive lesion". All clinically important lesions and their location, number, and size were recorded. Lesion conspicuity and visibility of normal abdominal structures (liver, adrenals, pancreas, gallbladder, kidneys, peritoneum, retroperitoneum, bowel, lymph node, ovary, uterus, and urinary bladder) were assessed using a 3-point scale [1 = sufficient (image quality sufficient for clinical diagnostic confidence), 2 = limited (image quality limited for clinical diagnostic confidence), 3 = unacceptable (image quality unacceptable for clinical diagnostic confidence)]. Image noise and artifacts were assessed on 3-pont scale (1 = no effect, 2 = limited effect, 3 = significant effect on clinical diagnostic confidence).

### *Objective image noise*

Objective image noise was measured on DICOM image viewer. A circular region of interest (ROI, 30 $mm^2$) was placed on the homogeneous area of liver parenchyma; CT numbers (Hounsfield Unit) and their standard deviations (image noise) were recorded for SD and all RD IRTs series.

### *Statistical analysis*

Data were analyzed using statistical software (SPSS 21, IBM, Armonk, NY). Subjective image quality scores were analyzed by Wilcoxon signed rank test. Analysis

**Table 1 Mean age, weight, body mass index, and effective diameter for vendor A, B and C**

| | Vendor A | Vendor B | Vendor C |
|---|---|---|---|
| Age (yr) | 60 ± 13 | 63 ± 12 | 58 ± 13 |
| weight (kg) | 84 ± 18 | 75 ± 16 | 89 ± 24 |
| BMI (kg/m$^2$) | 28 ± 5 | 27 ± 5 | 30 ± 8 |
| Effective diameter (cm) | 31 ± 4 | 30 ± 4 | 31 ± 5 |

BMI: Body mass index.

of variance tests were performed to compare objective image noise and CT number for all RD CT image series. The post hoc analysis was also performed. The *P*-value of $\leqslant$ 0.05 was considered statistically significant. Inter-observer variability was assessed using the kappa (k) value, categorized as poor < 0.2, fair 0.2-0.4, moderate 0.4-0.6, good 0.6-0.8, and very good 0.8-1. The statistical methods of this study were reviewed by Dr. Kalra from Massachusetts General Hospital.

## RESULTS

Continuous variables were expressed as mean ± standard deviation. The mean age, weight, BMI, and effective diameter for vendor A, B, and C are summarized in Table 1. The mean $CTDI_{vol}$, DLP, and estimated effective dose of SD and RD CT for vendor A, B, and C were summarized in Table 2. There was no significant difference in the BMI of patients among the three vendors (*P* = 0.6). In addition, there was no significant difference in the $CTDI_{vol}$ of RD CT (also SD CT) among the vendor A, B, and C.

### *Subjective image quality*

**Vendor A:** The subjective image quality scores are summarized in Table 3. There were total 50 "true positive" lesions on SD CT including kidney cysts (*n* = 15), liver cyst (*n* = 11), gall stones (*n* = 4), diverticulosis (*n* = 5), fatty liver (*n* = 3), kidney stone (*n* = 1), focal pancreatic lesion (*n* = 1), splenomegaly (*n* = 1), and other lesions (*n* = 9) such as lymph nodes, paracolonic abscess, low attenuating liver lesion, lytic lesion, and renal mass. On RD CT regardless of IRTs, 13 lesions were missed including kidney cysts (*n* = 4, < 3 mm), liver cyst (*n* = 3, 3-5 mm), and other lesions (*n* = 6) gall stone (< 3 mm), kidney stone (< 3 mm) (Figure 1), paracolonic abscess (< 8 mm), liver lesion (< 3 mm), focal pancreatic lesion, and lymph node. Lesions were missed regardless of effective diameter (30 cm, *P* = 0.5), BMI (27 kg/m$^2$, *P* = 0.3) of patients, and employed IRTs. There were also five pseudo lesions which include liver lesions (*n* = 3, 2-4 mm), renal stone (< 3 mm) (Figure 1), and diverticulosis (< 4 mm) on RD CT images.

Lesions conspicuity was sufficient for diagnostic performance for 6/24 lesions with RD A-1, 10/24 lesions with RD A-2, and 7/24 lesions with RD A-3 (*P* = 0.7). The liver margin was sufficiently seen in 14/22 patients with RD A-1, 16/22 patients with RD A-2 and, 13/22 patients with RD A-3. Visibility of liver parenchyma was limited for diagnostic performance in 22/22 patients with RD A-1, 17/22 patients with RD A-2, and 20/22 patients with RD A-3 (Figure 1). Renal parenchyma was not optimally seen on RD images regardless of IRTs. Visibility of other abdominal structures such as adrenal glands, bowels, peritoneum, and urinary bladder was not sufficient for diagnostic confidence on all RD IRTs. Subjective image noise and artifacts significantly affect the clinical diagnostic confidence of patient with greater body size (BMI >30 kg/m$^2$). Blotchy pixelated appearance was more common on RD A-1 images compared to RD A-2 and A-3. Interobserver agreement for subjective image quality was moderate (k = 0.43-0.57).

**Vendor B:** The subjective image quality scores are summarized in Table 4. Of 57 "true positive" on SD CT, there were kidney cysts (*n* = 23), liver cysts (*n* = 8), indeterminate liver lesions (*n* = 3), cholelithiasis (*n* = 3), diverticulosis (*n* = 6), fatty liver (*n* = 3), hernias (*n* = 4), pancreatic lesions (*n* = 2), splenomegaly (*n* = 1), and other lesions (*n* = 4) (lymph nodes, adrenal nodule, and enlarged prostate). There were 18 missed lesions on RD CT which included kidney cysts (*n* = 10, 2-4 mm), liver cysts (*n* = 2, 3-5 mm), and other missed lesions (*n* = 6) including gall stones (2-3 mm) (Figure 2), gall bladder nodule, ovarian cyst, liver lesion, fatty liver, and diverticulosis. Effective diameter (30 cm, *P* = 0.8) and BMI (27 kg/m$^2$, *P* = 0.5) of patients with missed lesions were not significantly different compared to that of the patients without missed lesions (29 cm and 27 kg/m$^2$). There were also four pseudo lesions including liver lesions (*n* = 2, < 3 mm), kidney cyst (< 3 mm) and diverticulosis (< 4 mm) on RD CT images.

Only 5/26 lesions were sufficiently seen on RD B-1, 6/26 lesions on RD B-2, and 7/26 lesions on RD B-3 images (*P* = 0.9). Liver margin was optimally seen in 10/22 patients with RD B-1 and RD B-2, and 11/22 patients with RD B-3. Visibility of liver and renal parenchyma was limited for diagnostic confidence for all patients regardless of IRTs (Figure 2). Visibility of other abdominal structures such as adrenals, gall bladder, bowels, peritoneum, and urinary bladder was not optimally seen on RD CT images. Ring artifacts (pelvic region) were noted on RD CT images of larger size patients (BMI > 30 kg/m$^2$) and were more prominent on RD B-2 images than RD B-1 and RD B-3 images. Also RD B-2 images were blotchy in appearance. Interobserver agreement for subjective image quality among was fair to moderate (k = 0.34-0.55).

**Vendor C:** The subjective image quality scores are summarized in Table 5. There were 40 "true positive" lesions detected on SD CT, including liver cysts (*n* = 9), kidney cysts (*n* = 7), gall stones (*n* = 2), diverticulosis (*n* = 3), fatty liver (*n* = 2), fluid collections (*n* = 3), pancreatic lesions (*n* = 2), hernias (*n* = 2), splenomegaly (*n* = 1), and other lesions (*n* = 9) including lymph nodes, diverticulitis, liver lesion, adrenal nodule, and urinary bladder diverticulum. Nine lesions were missed on RD CT

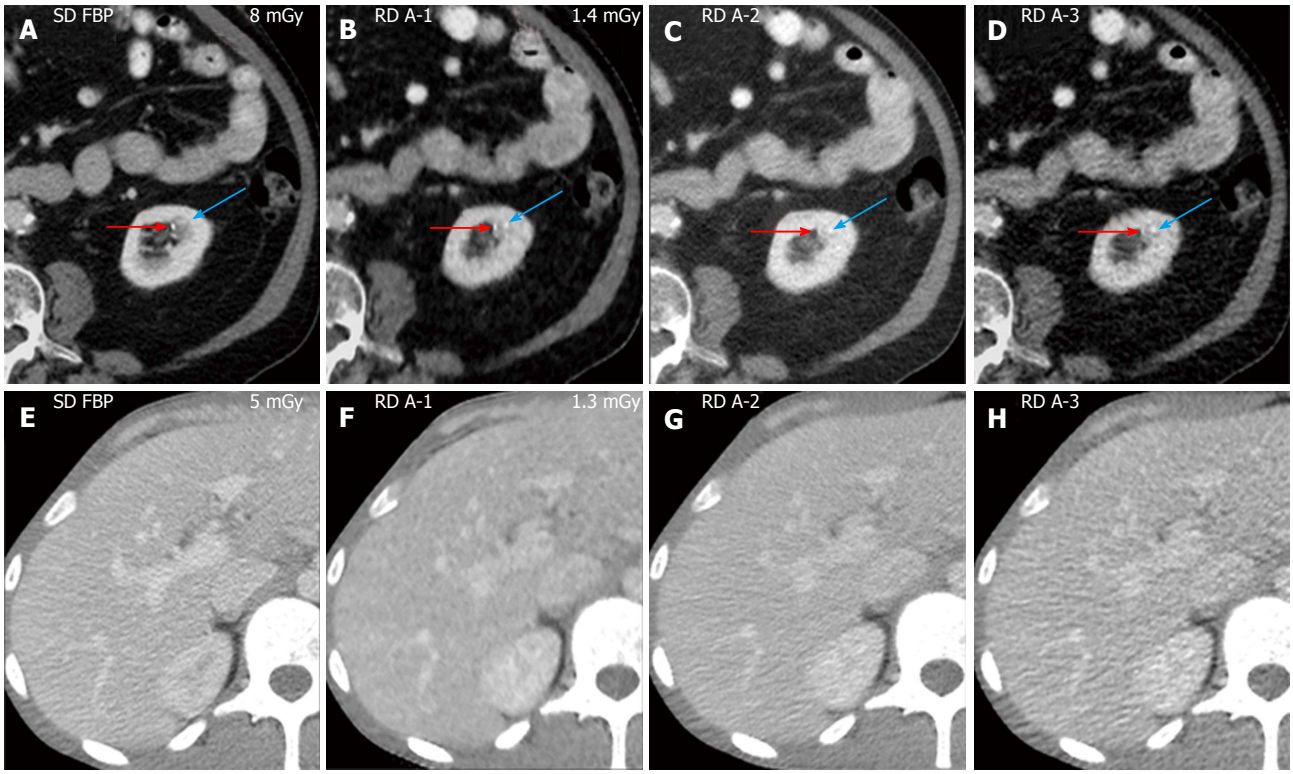


**Figure 1 Top row (A-D) and bottom row (E-H) of a 71-year-old male.** A-D: Transverse abdominal CT images of a 71-year-old male (BMI 24 kg/m$^2$) acquired at SD FBP (8 mGy) and RD (1.4 mGy) (reconstructed with A-1, A-2, and A-3). The left kidney stone (red arrows) was optimally depicted on SD FBP (A). However, left kidney stone was missed on RD A-1, RD A-2, and RD A-3 images (B-D). In addition, probably pseudo kidney stone (blue arrows) was seen on RD A-1, RD A-2, and RD A-3 images; E-H: Transverse abdominal CT images of a 3-year-old male (BMI 20 kg/m$^2$) acquired at SD FBP (5 mGy) and RD (1.3 mGy) reconstructed with A-1, A-2, and A-3. The liver parenchyma was optimally depicted on SD FBP, scored sufficiently on RD A-2, and limited on RD A-1 and RD A-3 images. SD: Standard of care; FBP: Filtered back projection; RD: Reduced dose; BMI: Body mass index; CT: Computed tomography.

**Table 2 Mean computed tomography dose index volume, dose length product, and estimated effective dose for standard of care and reduced dose computed tomography for vendor A, B and C**

| | Vendor A | | Vendor B | | Vendor C | | *P* value |
|---|---|---|---|---|---|---|---|
| | SD | RD | SD | RD | SD | RD | |
| $CTDI_{vol}$ (mGy) | 10 ± 3.4 | 1.2 ± 0.1 | 10 ± 3.4 | 1.3 ± 0.1 | 9 ± 5.3 | 1.4 ± 0.1 | < 0.001 |
| DLP (mGy*cm) | 483 ± 187 | 64 ± 2 | 426 ± 204 | 61 ± 3 | 386 ± 259 | 61 ± 3 | < 0.001 |
| Estimated effective dose (mSv) | 7 ± 3 | 0.9 ± 0.1 | 6 ± 3 | 0.9 ± 0.1 | 6 ± 4 | 0.9 ± 0.1 | < 0.001 |

DLP: Dose length product; $CTDI_{vol}$: Computed tomography dose index volume; SD: Standard of care; RD: Reduced dose.

regardless of IRTs including liver cysts (*n* = 3, 3-5 mm), gall stone (*n* = 2, < 8 mm) (Figure 3), pancreatitis (*n* = 1), and other missed lesions (*n* = 3, 2-6 mm) including kidney cyst, fluid collection, and lymph node. Effective diameter (32 cm, *P* = 0.7) and BMI (29 kg/m$^2$, *P* = 0.9) of patients with missed lesions were not significantly different than other patients (31 cm and 29 kg/m$^2$). There were also four pseudo lesions including two liver lesions (3-4 mm), kidney cyst (< 3 mm), and gall stone (< 3 mm) and regardless of IRTs.

Lesion conspicuity was acceptable in 4/20 lesions with RD C-1, 6/20 lesions with RD C-2, and 10/20 lesions with RD C-3. Lesion margin was better seen on 7/22 patients with RD C-1, 10/22 patients with RD C-2, and 13/22 patients with RD C-3 (*P* = 0.8). Liver and kidney parenchyma were not sufficiently seen in most patients with RD IRTs (Figure 3). Also visibility of other abdominal structures (adrenals, gall bladder, bowels, peritoneum, and urinary bladder) was not sufficient for diagnostic confidence at RD CT regardless of IRTs. Patients with a greater body size (> 30 kg/m$^2$) associated with more image noise and artifacts that can affect the diagnostic confidence. Interobserver agreement for subjective image quality among was moderate (k = 0.41-0.55).

### *Objective image quality*

Mean HU values and objective image noise are summarized in Table 6. There was no significant difference in CT numbers across respective IRTs (*P* = 0.9) of all vendors. Mean objective image noise in liver was significantly lower for RD A-1 compared to both RD A-2 and RD A-3 images (*P* < 0.001). Similarly, mean objective image noise lower for RD B-2 (compared to RD B-1, RD B-3) and RD C-3 (compared to RD C-1 and C-2) (*P* = 0.016).

**Table 3 Subjective image quality scores for reduced dose A-1, reduced dose A-2, and reduced dose A-3**

| | A-1 | | A-2 | | A-3 | |
|---|---|---|---|---|---|---|
| Reader 1 | | | | | | |
| Lesions | 1 (7/24) | 2 (16/24) | 1 (10/24) | 2 (13/24) | 1 (7/24) | 2 (15/24) |
| | 3 (1/24) | | 3 (1/24) | | 3 (2/24) | |
| Liver margins | 1 (18/22) | 2 (4/22) | 1 (20/22) | 2 (2/22) | 1 (17/22) | 2 (5/22) |
| Liver parenchyma | 1 (4/22) | 2 (15/22) | 1 (7/22) | 2 (14/22) | 1 (5/22) | 2 (15/22) |
| | 3 (3/22) | | 3 (1/22) | | 3 (2/22) | |
| Adrenals bowels | 1 (7/22) | 2 (15/22) | 1 (11/22) | 2 (11/22) | 1 (8/22) | 2 (14/22) |
| | 1 (7/22) | 2 (14/22) | 1 (10/22) | 2 (12/22) | 1 (8/22) | 2 (14/22) |
| | 3 (1/23) | | | | | |
| Reader 2 | | | | | | |
| Lesions | 1 (5/25) | 2 (17/25) | 1 (8/25) | 2 (12/25) | 1 (7/25) | 2 (13/25) |
| | 3 (3/25) | | 3 (5/25) | | 3 (5/25) | |
| Liver margins | 1 (10/22) | 2 (11/22) | 1 (12/22) | 2 (10/22) | 1 (9/22) | 2 (13/22) |
| | 3 (1/22) | | | | | |
| Liver parenchyma | 1 (2/22) | 2 (8/22) | 1 (2/22) | 2 (10/22) | 1 (2/22) | 2 (10/22) |
| | 3 (12/22) | | 3 (10/22) | | 3 (10/22) | |
| Adrenals | 1 (7/22) | 2 (12/22) | 1 (9/22) | 2 (11/22) | 1 (7/22) | 2 (13/22) |
| | 3 (3/22) | | 3 (2/22) | | 3 (2/22) | |
| Bowels | 1 (12/22) | 2 (8/22) | 1 (12/22) | 2 (8/22) | 1 (10/22) | 2 (10/22) |
| | 3 (3/22) | | 3 (2/22) | | 3(2/22) | |

Score (seen by number of lesions or patients/total number of lesions or patients), score of 1 = sufficient, 2 = limited, 3 = unacceptable for clinical diagnostic confidence.

**Table 4 Subjective image quality scores for reduced dose B-1, reduced dose B-2, and reduced dose B-3**

| | B-1 | | B-2 | | B-3 | |
|---|---|---|---|---|---|---|
| Reader 1 | | | | | | |
| Lesions | 1 (4/27) | 2 (22/27) | 1 (4/27) | 2 (19/27) | 1 (7/27) | 2 (18/27) |
| | 3 (1/27) | | 3 (4/27) | | 3 (2/27) | |
| Liver margins | 1 (14/22) | 2 (8/22) | 1 (12/22) | 2 (10/22) | 1 (16/22) | 2 (6/22) |
| Liver parenchyma | 1 (1/22) | 2 (16/22) | 1 (1/22) | 2 (14/22) | 1 (1/22) | 2 (16/22) |
| | 3 (5/22) | | 3 (7/22) | | 3 (5/22) | |
| Adrenals | 1 (2/22) | 2 (14/22) | 1 (2/22) | 2 (13/22) | 1 (3/22) | 2 (15/22) |
| | 3 (6/22) | | 3 (7/22) | | 3 (4/22) | |
| Bowels | 3 (7/23) | 2 (15/22) | 3 (7/23) | 2 (15/22) | 3 (6/23) | 2 (16/22) |
| Reader 2 | | | | | | |
| Lesions | 1 (5/30) | 2 (19/30) | 1 (8/30) | 2 (18/28) | 1 (7/30) | 2 (15/30) |
| | 3 (6/30) | | 3 (4/30) | | 3 (8/30) | |
| Liver margins | 1 (6/22) | 2 (14/22) | 1 (8/22) | 2 (13/22) | 1 (6/22) | 2 (14/22) |
| | 3 (2/22) | | 3 (1/22) | | 3 (2/22) | |
| Liver parenchyma | 3 (17/22) | 2 (5/22) | 3 (16/22) | 2 (6/22) | 3 (18/22) | 2 (4/22) |
| Adrenals | 1 (3/22) | 2 (10/22) | 1 (4/22) | 2 (11/22) | 1 (2/22) | 2 (9/22) |
| | 3 (9/22) | | 3 (7/22) | | 3 (11/22) | |
| | 3 (4/22) | | 3 (1/22) | | 3 (5/22) | |
| Bowels | 1 (4/22) | 2 (16/22) | 1 (5/22) | 2 (16/22) | 1 (3/22) | 2 (17/22) |
| | 3 (2/22) | | 3 (1/22) | | 3 (2/22) | |

Score (seen by number of lesions or patients/total number of lesions or patients), score of 1 = sufficient, 2 = limited, 3 = unacceptable for clinical diagnostic confidence.

## DISCUSSION

We noted missed (2-7 mm) and pseudo (2-3 mm) lesions on abdominal CT acquired at $CTDI_{vol}$ of 1.3 mGy for all vendors regardless of employed IRTs and size of patients (based on effective diameter and BMI). Lesion conspicuity of most lesions (including renal and gall stones) was also limited for diagnostic confidence at 1.3 mGy with all assessed IRTs. These limitations with lesion detection and lesion conspicuity were observed despite the difference in subjective image quality for different vendors. Some IRTs (such as RD A-2, RD B-3, and RD C-3) improved the lesion conspicuity and visibility of abdominal structures compared to other IRTs in their respective group, although these improvements were not statistically significant ($P$ = 0.9). Likewise, although there was substantial ($P$ = 0.02) lower objective image noise with some IRTs (RD A-1, RD B-2, and RD C-3) compared to other IRTs in their group but this did not improve the readers' ability to detect or assess

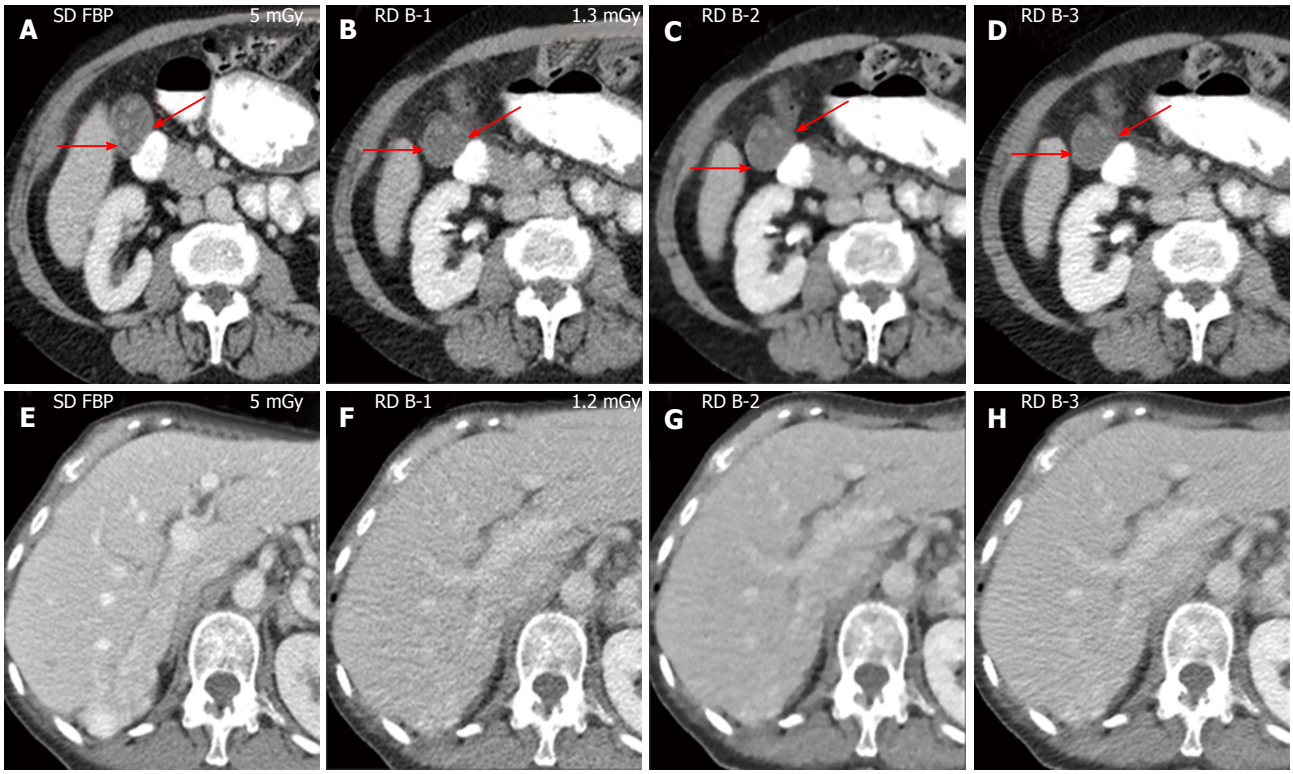


**Figure 2 Top row (A-D) and bottom (E-H) row of a 68-year-old female.** A-D: Transverse abdominal CT images of a 68-year-old female (BMI 25 kg/m$^2$) acquired at SD FBP (5 mGy) and RD (1.3 mGy) (reconstructed with B-1, B-2, and B-3). The gall bladder stones (arrows) were optimally depicted on SD FBP but missed on RD B-1, RD B-2, and RD B-3 images; E-H: Transverse abdominal CT images of a 71-year-old female (BMI 25 kg/m$^2$) acquired at SD FBP (5 mGy) and RD (1.2 mGy) (reconstructed with B-1, B-2, and B-3). The liver parenchyma was optimally depicted on SD FBP, scored sufficiently on RD B-3, and limited on RD B-1 and RD B-2 images. SD: Standard of care; FBP: Filtered back projection; RD: Reduced dose; BMI: Body mass index; CT: Computed tomography.

**Table 5 Subjective image quality scores for reduced dose C-1, reduced dose C-2, and reduced dose C-3**

| | C-1 | | C-2 | | C-3 | |
|---|---|---|---|---|---|---|
| Reader 1 | | | | | | |
| Lesions | 1 (2/19) | 2 (11/19) | 1 (5/19) | 2 (10/19) | 1 (7/19) | 2 (9/19) |
| | 3 (6/19) | | 3 (4/19) | | 3 (3/19) | |
| Liver margins | 1 (8/22) | 2 (14/22) | 1 (13/22) | 2 (9/22) | 1 (16/22) | 2 (6/22) |
| Liver parenchyma | 1 (1/22) | 2 (13/22) | 1 (2/22) | 2 (14/22) | 1 (2/22) | 2 (17/22) |
| | 3 (8/22) | | 3 (6/22) | | 3 (3/22) | |
| Adrenals | 1 (4/22) | 2 (13/22) | 1 (5/22) | 2 (14/22) | 1 (7/22) | 2 (12/22) |
| | 3 (5/22) | | 3 (3/22) | | 3 (3/22) | |
| Bowels | 1 (4/22) | 2 (14/22) | 1 (4/22) | 2 (13/22) | 1 (5/22) | 2 (14/22) |
| | 3 (4/23) | | 3 (5/23) | | 3 (3/23) | |
| Reader 2 | | | | | | |
| Lesions | 1 (6/20) | 2 (9/20) | 1 (7/20) | 2 (10/20) | 1 (13/20) | 2 (6/20) |
| | 3 (5/20) | | 3 (3/20) | | 3 (1/20) | |
| Liver margins | 1 (6/22) | 2 (12/22) | 1 (7/22) | 2 (11/22) | 1 (9/22) | 2 (11/22) |
| | 3 (4/22) | | 3 (4/22) | | 3 (2/22) | |
| Liver parenchyma | 1 (2/22) | 2 (5/22) | 1 (3/22) | 2 (6/22) | 1 (4/22) | 2 (5/22) |
| | 3 (15/22) | | 3 (13/22) | | 3 (13/22) | |
| Adrenals | 1 (5/22) | 2 (8/22) | 1 (6/22) | 2 (7/22) | 1 (9/22) | 2 (6/22) |
| | 3 (10/22) | | 3 (9/22) | | 3 (7/22) | |
| Bowels | 1 (10/22) | 2 (10/22) | 1 (12/22) | 2 (8/22) | 1 (13/22) | 2 (8/22) |
| | 3 (2/22) | | 3 (2/22) | | 3 (1/22) | |

Score (seen by number of lesions or patients/total number of lesions or patients) score of 1 = sufficient, 2 = limited, 3 = unacceptable for clinical diagnostic confidence.

the abdominal abnormalities. The unreliability of noise reduction to predict lesion evaluability on RD-CT has also been reported in prior publications[12,13]. Pourjabbar *et al*[13] have reported that IRT settings with greater noise reduction often provide suboptimal image quality in terms of loss of sharpness and visibility of lesion margins.

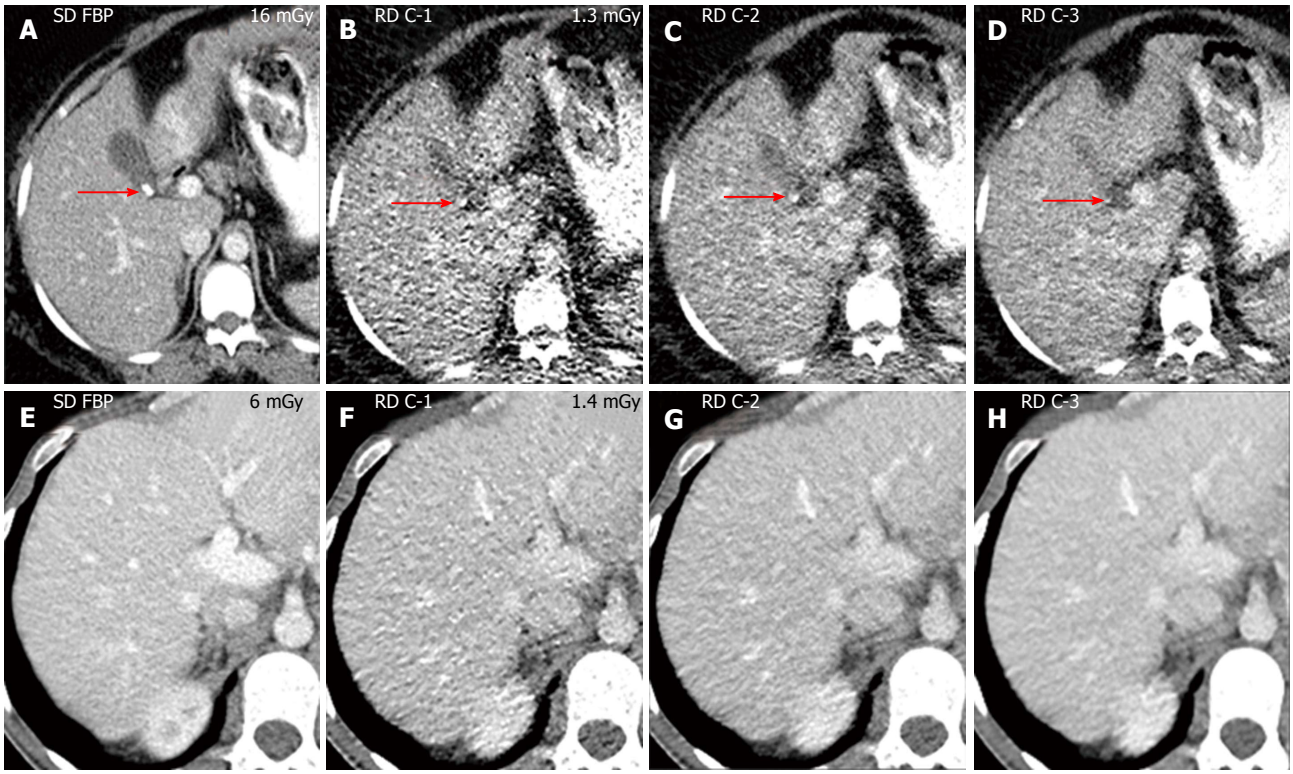


**Figure 3 Top row (A-D) and bottom row (E-H) of a 41-year-old female.** A-D: Transverse abdominal CT images of a 41-year-old female (BMI 38 kg/m$^2$) acquired at SD FBP (16 mGy) and RD (1.3 mGy) (reconstructed with C-1, C-2, and C-3). The gall bladder stone (arrows) was optimally depicted on SD FBP. However, gall bladder stone was missed on RD C-1, RD C-2, and RD C-3 images; E-H: Transverse abdominal CT images of a 29-year-old male (BMI 18 kg/m$^2$) acquired at SD FBP (6 mGy) and RD (1.4 mGy) (reconstructed with C-1, C-2, and C-3). The liver parenchyma was optimally depicted on SD FBP, scored sufficiently on RD C-3, and limited on RD C-1 and RD C-2 images. SD: Standard of care; FBP: Filtered back projection; RD: Reduced dose; BMI: Body mass index; CT: Computed tomography.

**Table 6 Mean HU values and objective image noise in region of interest placed in liver for standard of care filtered back projection and reduced dose iterative reconstruction techniques**

| | | HU values | Objective image noise |
|---|---|---|---|
| Vendor A | SD FBP | 104 ± 30 | 17 ± 3 |
| | RD A-1 | 93 ± 35 | 16 ± 4 |
| | RD A-2 | 97 ± 29 | 19 ± 4 |
| | RD A-3 | 98 ± 29 ($P$ = 0.9) | 24 ± 5 ($P$ < 0.001) |
| Vendor B | SD FBP | 101 ± 28 | 26 ± 5 |
| | RD B-1 | 100 ± 25 | 29 ± 5 |
| | RD B-2 | 98 ± 24 | 14 ± 3 |
| | RD B-3 | 107 ± 23 ($P$ = 0.3) | 33 ± 11 ($P$ < 0.001) |
| Vendor C | SD FBP | 103 ± 28 | 23 ± 7 |
| | RD C-1 | 97 ± 26 | 36 ± 18 |
| | RD C-2 | 97 ± 26 | 28 ± 14 |
| | RD C-3 | 98 ± 25 ($P$ = 0.9) | 23 ± 11 ($P$ = 0.016) |

FBP: Filtered back projection; SD: Standard of care; RD: Reduced dose.

Pooler *et al*[14] reported that renal stones (> 4 mm) can be detected at 1.3 mGy (0.9 mSv) with adaptive statistical iterative reconstruction (ASIR, GE Healthcare, Waukesha, WI) and model based iterative reconstruction (MBIR, GE Healthcare). They also reported missed renal stones on ASIR and MBIR images but pseudo renal stones were seen only on ASIR images. Vardhanabhuti *et al*[15] have also reported missed liver lesions on RD ASIR and MBIR images at 2.3 mGy (which is higher than radiation dose used in our study, 1.3 mGy). They concluded that despite extensive noise reduction, diagnostic confidence of MBIR was suboptimal compared to ASIR. Padole *et al*[16] also reported missed lesions at 1.3 mGy with FBP, ASIR, and MBIR regardless of size of patients. The more number of false and missed lesions in our study as compared to prior studies[14,15] may have resulted from inclusion of all abdominal abnormities in our study as assessed for interpretation of routine abdominal CT.

Some of the results of our study were in contradiction with prior publications[17,18]. Yasaka *et al*[17] have reported detection of adrenal nodules detection was not compromised at 0.7 mGy CT examination reconstructed with MBIR images. We missed several abdominal abnormalities with multiple IRTs at higher $CTDI_{vol}$ of 1.3 mGy. This could have resulted from difference in the patient size between our (average weight 75 ± 16 kg) and prior study (average weight 61 ± 12 kg). Khawaja *et al*[18] reported uncompromised abdominal lesion detection at 1.3 mGy (0.9 mSv) with IMR (Philips Healthcare, Netherlands). This study employed a side-by-side comparison of RD-IRTs and SD CT which can bias the radiologists in terms of lesion detection, whereas in our study independent, unbiased assessment of different RD-IRTs was performed. Importantly, in the study from Khawaja *et al*[18] there was noticeable decrease in subjective image quality as well as lesion conspicuity

which is in agreement with our study. The prior studies showed acceptable image quality for abdominal CT acquired at $CTDI_{vol}$ of 3-4 mGy with IRTs[5,12,15].

Even though most liver and renal lesions were detected on RD CT images in our study, visibility of normal liver and renal parenchyma was not sufficient for diagnostic confidence for all vendors on RD CT regardless of IRTs. We also noticed more pseudo lesions in liver and renal parenchyma. Pseudo lesions noted in our study on these structures on RD CT could have been due to multiple reasons including partial volume averaging effect, image artifacts, or both. These pseudo lesions were most prominently seen on IRTs with greater noise reduction. We have also reported blotchy pixelated appearance with some IRTs at lower image noise. Thus, IRTs with greater noise reduction potential could have changed the texture of images and made these pseudo lesions more prominent. This also may have contributed to inferior performance of some IRTs compared to other IRTs. We have also noticed that the ring artifacts, particularly with larger size patients which may have been due to photon starvation phenomenon associated with low energy photons.

Major implication of our study is that abdominal CT acquired at 1.3 mGy (or at sub-milli-sievert level) is not sufficient to assess the abdominal lesions and structures even with the MDCT scanners of different vendors and IRTs (vendor specific and neutral) assessed in our study. Also, objective image noise is not a reliable factor for the improvement of image quality with IRTs on RD CT. Our study emphasize need for continue improvement in CT hardware/software technology by all CT vendors for attaining the goal of sub-milli-sievert abdominal CT[19].

There were few limitations of our study. First, sample size of our study was small comprising 66 patients only. Second, we acquired RD CT without additional contrast; hence there was some difference in the contrast enhancement of SD and RD CT images. This difference was minimized by immediate (within 5-10 s) acquisition of RD CT followed by SD CT. Third, in order to achieve the sub-milli-sievert (0.9 mSv), we scanned all size patients (RD CT) with fixed tube current, hence effect of AEC was not assessed in our study. Also, this sub-milli-sievert dose may not be sufficient to assess abdominal CT in routine clinical settings. Fourth, due to blinding of study, we did not know the performance of specific vendor or RD IRTs.

In conclusion, regardless of the iterative reconstruction techniques and MDCT vendors, abdominal CT acquired at mean $CTDI_{vol}$ 1.3 mGy (at sub-mill-sievert) radiation dose was not sufficient to retain clinical diagnostic performance. Lesion evaluation is compromised at sub-milli-sievert doses in abdomen regardless of CT vendor and IRTs. Sufficient clinical diagnostic confidence can be achieved at 3-4 mGy for abdominal CT[5,12,15]. In order to achieve sub-milli-sievert doses (1.3 mGy) in abdomen, CT vendors and users should develop new groundbreaking technologies in both CT hardware and image processing domains.

## COMMENTS

### Background

Computed tomography (CT) radiation dose is a vital. Several strategies including improvement in image reconstruction with iterative reconstruction techniques (IRT) have been implemented to reduce CT radiation dose. In this study, the authors assessed the performance IRTs for abdominal CT acquired at sub-milli-Sievert radiation dose.

### Research frontiers

The authors' study emphasize need for continue improvement in CT hardware/software technology by all CT vendors for attaining the goal of sub-milli-Sievert abdominal CT.

### Innovations and breakthroughs

In this study, the authors compared the clinical diagnostic performance of vendor specific and vendor neutral IRTs of different multi-detector CT (MDCT) ($\geqslant$ 64 row) vendors at sub-milli-Sievert radiation dose to the standard of care abdominal CT.

### Applications

Major implication of the authors' study is that abdominal CT acquired at sub-milli-sievert radiation dose is not sufficient to assess the abdominal lesions and structures even with the MDCT scanners of different vendors and IRTs (vendor specific and neutral) assessed in the authors'study.

### Terminology

The filtered back projection algorithm uses several fundamental assumptions about CT scanner geometry for image reconstruction which may have faster reconstruction time but higher image noise. The IRT algorithm (computationally more complex) uses different assumptions about CT scanner geometry with multiple iterations for image reconstruction which may have longer reconstruction time but lower image noise.

### Peer-review

This paper compared the image quality of reduced dose abdominal CT with 9 reconstruction techniques from 4 different vendors. They concluded that mean $CTDI_{vol}$ 1.3 mGy is not sufficient for clinical diagnostic performance.This work is up to the level of the journal.

## REFERENCES


1 **Schauer DA**, Linton OW. National Council on Radiation Protection and Measurements report shows substantial medical exposure increase. *Radiology* 2009; **253**: 293-296 [PMID: 19864524 DOI: 10.1148/radiol.2532090494]

2 **Kalra MK**, Maher MM, Toth TL, Hamberg LM, Blake MA, Shepard JA, Saini S. Strategies for CT radiation dose optimization. *Radiology* 2004; **230**: 619-628 [PMID: 14739312]

3 **Hricak H**, Brenner DJ, Adelstein SJ, Frush DP, Hall EJ, Howell RW, McCollough CH, Mettler FA, Pearce MS, Suleiman OH, Thrall JH, Wagner LK. Managing radiation use in medical imaging: a multifaceted challenge. *Radiology* 2011; **258**: 889-905 [PMID: 21163918 DOI: 10.1148/radiol.10101157]

4 **Singh S**, Kalra MK, Ali Khawaja RD, Padole A, Pourjabbar S, Lira D, Shepard JA, Digumarthy SR. Radiation dose optimization and thoracic computed tomography. *Radiol Clin North Am* 2014; **52**: 1-15 [PMID: 24267707 DOI: 10.1016/j.rcl.2013.08.004]

5 **Singh S**, Kalra MK, Hsieh J, Licato PE, Do S, Pien HH, Blake MA. Abdominal CT: comparison of adaptive statistical iterative and filtered back projection reconstruction techniques. *Radiology* 2010; **257**: 373-383 [PMID: 20829535 DOI: 10.1148/radiol.10092212]

6 **Singh S**, Kalra MK, Do S, Thibault JB, Pien H, O'Connor OJ, Blake MA. Comparison of hybrid and pure iterative reconstruction techniques with conventional filtered back projection: dose reduction potential in the abdomen. *J Comput Assist Tomogr* 2012; **36**: 347-353 [PMID: 22592622 DOI: 10.1097/RCT.0b013

e31824e639e]
7 **Vardhanabhuti V**, Loader RJ, Mitchell GR, Riordan RD, Roobottom CA. Image quality assessment of standard- and low-dose chest CT using filtered back projection, adaptive statistical iterative reconstruction, and novel model-based iterative reconstruction algorithms. *AJR Am J Roentgenol* 2013; **200**: 545-552 [PMID: 23436843 DOI: 10.2214/AJR.12.9424]
8 **Volders D**, Bols A, Haspeslagh M, Coenegrachts K. Model-based iterative reconstruction and adaptive statistical iterative reconstruction techniques in abdominal CT: comparison of image quality in the detection of colorectal liver metastases. *Radiology* 2013; **269**: 469-474 [PMID: 23847252 DOI: 10.1148/radiol.13130002]
9 **Kulkarni NM**, Uppot RN, Eisner BH, Sahani DV. Radiation dose reduction at multidetector CT with adaptive statistical iterative reconstruction for evaluation of urolithiasis: how low can we go? *Radiology* 2012; **265**: 158-166 [PMID: 22891359]
10 **Christner JA**, Kofler JM, McCollough CH. Estimating effective dose for CT using dose-length product compared with using organ doses: consequences of adopting International Commission on Radiological Protection publication 103 or dual-energy scanning. *AJR Am J Roentgenol* 2010; **194**: 881-889 [PMID: 20308486 DOI: 10.2214/AJR.09.3462]
11 **AAPM Task Group**. Size-specific dose estimates (SSDE) in pediatric and adult body 324 325 CT Examinations: report of AAPM Task Group 204. [updated 2014 Jun 20]. Available from: URL: http//www.aapm.org/pubs/reports/rpt_204
12 **Kalra MK**, Woisetschläger M, Dahlström N, Singh S, Lindblom M, Choy G, Quick P, Schmidt B, Sedlmair M, Blake MA, Persson A. Radiation dose reduction with Sinogram Affirmed Iterative Reconstruction technique for abdominal computed tomography. *J Comput Assist Tomogr* 2012; **36**: 339-346 [PMID: 22592621 DOI: 10.1097/RCT.0b013e31825586c0]
13 **Pourjabbar S**, Singh S, Singh AK, Johnston RP, Shenoy-Bhangle AS, Do S, Padole A, Blake MA, Persson A, Kalra MK. Preliminary results: prospective clinical study to assess image-based iterative reconstruction for abdominal computed tomography acquired at 2 radiation dose levels. *J Comput Assist Tomogr* 2014; **38**: 117-122 [PMID: 24424560 DOI: 10.1097/RCT.0b013e3182a17629]
14 **Pooler BD**, Lubner MG, Kim DH, Ryckman EM, Sivalingam S, Tang J, Nakada SY, Chen GH, Pickhardt PJ. Prospective trial of the detection of urolithiasis on ultralow dose (sub mSv) noncontrast computerized tomography: direct comparison against routine low dose reference standard. *J Urol* 2014; **192**: 1433-1439 [PMID: 24859440 DOI: 10.1016/j.juro.2014.05.089]
15 **Vardhanabhuti V**, Riordan RD, Mitchell GR, Hyde C, Roobottom CA. Image comparative assessment using iterative reconstructions: clinical comparison of low-dose abdominal/pelvic computed tomography between adaptive statistical, model-based iterative reconstructions and traditional filtered back projection in 65 patients. *Invest Radiol* 2014; **49**: 209-216 [PMID: 24368613 DOI: 10.1097/RLI.0000000000000017]
16 **Padole A**, Singh S, Lira D, Blake MA, Pourjabbar S, Khawaja RD, Choy G, Saini S, Do S, Kalra MK. Assessment of Filtered Back Projection, Adaptive Statistical, and Model-Based Iterative Reconstruction for Reduced Dose Abdominal Computed Tomography. *J Comput Assist Tomogr* 2015; **39**: 462-467 [PMID: 25734468 DOI: 10.1097/RCT.0000000000000231]
17 **Yasaka K**, Katsura M, Akahane M, Sato J, Matsuda I, Ohtomo K. Model-based iterative reconstruction for reduction of radiation dose in abdominopelvic CT: comparison to adaptive statistical iterative reconstruction. *Springerplus* 2013; **2**: 209 [PMID: 23687632 DOI: 10.1186/2193-1801-2-209]
18 **Khawaja RD**, Singh S, Blake M, Harisinghani M, Choy G, Karosmangulu A, Padole A, Do S, Brown K, Thompson R, Morton T, Raihani N, Koehler T, Kalra MK. Ultra-low dose abdominal MDCT: using a knowledge-based Iterative Model Reconstruction technique for substantial dose reduction in a prospective clinical study. *Eur J Radiol* 2015; **84**: 2-10 [PMID: 25458225 DOI: 10.1016/j.ejrad.2014.09.022]
19 **McCollough CH**, Chen GH, Kalender W, Leng S, Samei E, Taguchi K, Wang G, Yu L, Pettigrew RI. Achieving routine submillisievert CT scanning: report from the summit on management of radiation dose in CT. *Radiology* 2012; **264**: 567-580 [PMID: 22692035]

**P- Reviewer**: Cerwenka HR, Chow J
**S- Editor**: Qiu S **L- Editor**: A **E- Editor**: Li D

Published by **Baishideng Publishing Group Inc**
8226 Regency Drive, Pleasanton, CA 94588, USA
Telephone: +1-925-223-8242
Fax: +1-925-223-8243
E-mail: bpgoffice@wjgnet.com
Help Desk: http://www.wjgnet.com/esps/helpdesk.aspx
http://www.wjgnet.com